

# SCIENTIFIC REPORTS



OPEN

## Fabrication of Si negative electrodes for Li-ion batteries (LIBs) using cross-linked polymer binders

Suk-Yong Jang<sup>1</sup> & Sien-Ho Han<sup>2</sup>

Received: 13 July 2016

Accepted: 03 November 2016

Published: 19 December 2016

Currently, Si as an active material for LIBs has been attracting much attention due to its high theoretical specific capacity (3572 mAh g<sup>-1</sup>). However, a disadvantage when using a Si negative electrode for LIBs is the abrupt drop of its capabilities during the cycling process. Therefore, there have been a few studies of polymers such as poly(vinylidene fluoride) (PVdF), carboxymethyl cellulose (CMC), styrene butadiene rubber (SBR) and polyacrylic acid (PAA) given that the robust structure of a polymeric binder to LIBs anodes is a promising means by which to enhance the performance of high-capacity anodes. These studies essentially focused mainly on modifying of the linear-polymer component or on copolymers dissolved in solvents. Cross-linking polymers as a binder may be preferred due to their good scratch resistance, excellent chemical resistance and high levels of adhesion and resilience. However, because these types of polymers (with a rigid structure and cross-linking points) are also insoluble in general organic solvents, applying these types in this capacity is virtually impossible.

In theory, at least, a multifunctional monomer can easily cross-link by itself<sup>1-5</sup>, and our laboratory utilized pentaerythritol triacrylate (PETA), pentaerythritol tetraacrylate (PETTA) and dipentaerythritol pentaacrylate (DPEPA) multifunctional monomers containing three, four and five carbon-carbon double bonds at the backbone. The Si/carbon black (CB)/(poly)pentaerythritol triacrylate (PPETA) composite (PPETA-composite), Si/CB/(poly)pentaerythritol tetraacrylate (PPETTA) composite (PPETTA-composite) and Si/CB/(poly)dipentaerythritol pentaacrylate (PDPEPA) composite (PDPEPA-composite) were fabricated via a curing process from a Si/CB/pentaerythritol triacrylate (PETA) composite mixture (PETA-composite mixture), a Si/CB/pentaerythritol tetraacrylate (PETTA) composite mixture (PETTA-composite mixture) and a Si/CB/dipentaerythritol pentaacrylate (DPEPA) composite mixture (DPEPA-composite mixture), respectively<sup>2-4</sup>. The resulting charge (delithiation) rates were close to 4, 5 and 3 times higher than a Si/CB/PVdF composite containing the well-known PVdF binder for 15 cycles. Specifically, the discharge (lithiation) of the Si/CB/PVdF/PPETTA composite (1:2) (PVdF/PPETTA-composite (1:2)) (approximately 3013 mAh g<sup>-1</sup>) containing the PVdF/PPETTA (1:2) blended polymer (PVdF/PPETTA (1:2) binder) (blending ratio, 1.0/2.0) as a binder was improved by approximately 654 mAh g<sup>-1</sup> compared to the Si/CB/PVdF composite (PVdF-composite) (about 2359 mAh g<sup>-1</sup>). The purpose of this study was to determine whether a relationship exists between the application of a cross-linking polymer binder and the performance of Si negative electrodes for LIBs. Another objective was to present a novel process by which to fabricate Si negative electrodes for LIBs with a cross-linked polymer binder system. Figure 1 shows the cross-linking routes of the PETA, PETTA and DPEPA multifunctional monomers.

### Results and Discussion

**Fabrication of composite electrodes.** First, the PETA-composite mixture, the PETTA-composite mixture, the DPEPA-composite mixture and the PVdF/PETTA-composite mixtures were all fabricated by the direct mixing of 60% Si, 25% CB, 15% of a binder and 2,20-azobisisobutyronitrile (a radical initiator, AIBN) in N-methyl-2-pyrrolidone (NMP). Secondly, the composite mixtures were cast on a Cu-foil, and then cured in a silicon-packed mold for polymerization at 85 °C for 2 h<sup>3,4</sup>. Finally, the resulting composite electrodes were dried in a vacuum oven at 120 °C for 1 h. In order to enhance the inter-particle contact, the composite electrodes were roll-pressed. The entire fabrication process to create the PVdF/PPETTA-composites is shown in Fig. 2. The materials

<sup>1</sup>Graduate School of Knowledge Based Technology and Energy, Korea Polytechnic University 237 Sangdaehak-Ro (2121 Jungwang-Dong) Siheung-Si, Gyeonggi-Do 429-450, Republic of Korea. <sup>2</sup>Department of Chem. Eng. & Biotech., Korea Polytechnic University, 237 Sangdaehak-Ro, 2121 Jeongwang-Dong, Siheung-Si, Gyeonggi-Do 429-793, Republic of Korea. Correspondence and requests for materials should be addressed to S.Y.J. (email: jsy95@kpu.ac.kr) or S.H.H. (email: han@kpu.ac.kr)

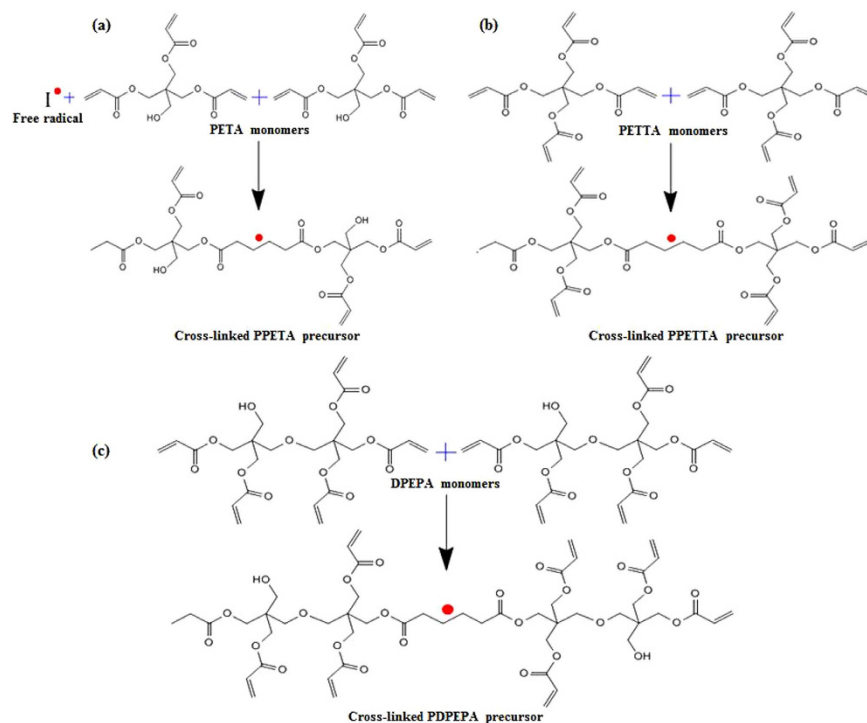


**Figure 1.** Cross-linking routes of the PETA (a), PETTA (b) and DPEPA (c) multifunctional monomers.

used for the fabrication of the PVdF-composite, PPETA-composite, PPETTA-composite, PDPEPA-composite and PVdF/PPETTA-composites are summarized in Table 1. Photographs of the PVdF-composite, PPETA-composite, PPETTA-composite, PDPEPA-composite and PVdF/PPETTA-composites are shown in Fig. 3. The cell production process used to create the composite electrodes is shown in Fig. 4. Images of the PVdF-composite, PPETA-composite, PPETTA-composite, PDPEPA-composite and PVdF/PPETTA-composites after 10 cycles are shown in Fig. 5.

**Fabrication of raw-binder samples.** The PETA, PETTA, DPEPA, PVdF/PETTA (1:1) mixture, PVdF/PETTA (1:2) mixture and PVdF/PETTA (1:5) mixture were dissolved in NMP to form the homogeneous solutions described in Table 2. Then, a radical initiator, AIBN, was added to the solutions and directly poured into a silicon-packed mold (size: 3.0 × 3.0 cm) to carry out cross-linking polymerization for 2 h at 85 °C. After the polymerization step was complete, raw PPETA, PPETTA, PDPEPA, PVdF/PPETTA (1:1), PVdF/PPETTA (1:2) and PVdF/PPETTA (1:5) binder samples with a thickness of about 0.2 cm were obtained. The resulting samples were dried in a vacuum oven at 120 °C for 1 h. The raw-PVdF binder sample was prepared by a solution casting method. The materials for the fabrication and the resulting electrolyte uptake (EU) of each raw-binder are summarized in Table 2.

**FE-SEM image of composite electrodes.** Figure 6 shows a FE-SEM image of the Si used in this study. The morphology of the Si in this case was highly irregular. The average particle size was approximately 10 μm. Figure 7 shows FE-SEM images of the PVdF-composite, the PPETTA-composite and the PVdF/PPETTA-composite (1:1). As shown in Fig. 7(a) 1 and 2, the surface of the PVdF-composite cracked frequently. In addition, the CB particles in this case were highly aggregated (Fig. 7(a) 3). However, there were far fewer, surface cracks in the PPETTA-composite (Fig. 7(b) 1,2) and the PVdF/PPETTA-composite (1:1) (Fig. 7(c) 1,2) compared to the PVdF-composite. The CB particles in these case (Fig. 7(b) 3 and (c) 3) were very well dispersed. Judging from this, the cross-link networks of the PPETTA as a binder played a role in reinforcing the binding strength between the electrode particles within the composite electrodes<sup>5,6</sup>. This most likely occurs because the CB particle inter-distances for the PPETTA-composite and the PVdF/PPETTA-composite (1:1) expanded as the PETTA monomer chains were extended through a curing process<sup>3-5</sup>.

**Electrolyte uptake (EU) of the binders.** Figure 8(a) shows the electrolyte uptake of the PVdF, PPETA, PPETTA, PDPEPA and PVdF/PPETTA binders. Interestingly, the electrolyte uptake levels for the PPETA, PPETTA and PDPEPA samples were approximately 154.4%, 188.5% and 98.2%, close to 8, 10 and 5 fold greater than that of the PVdF sample (approximately 18.9%) despite the fact that they are cross-linking polymers. The PPETTA sample had the best electrolyte uptake. Because the electrolyte solution is absorbed only into the hydrophobic segments<sup>4,5,7</sup>, we consider that the electrolyte uptake levels of the PPETA and PDPEPA samples containing the hydroxyl groups (–OH, hydrophilic segments) at the side chain were decreased compared to that of the PPETTA sample<sup>4,5,8</sup>. The corresponding electrolyte uptake levels of the PVdF/PPETTA (1:1), PVdF/PPETTA (1:2) and PVdF/PPETTA (1:5) binders were approximately 26.7%, 39.4% and 60.5%.

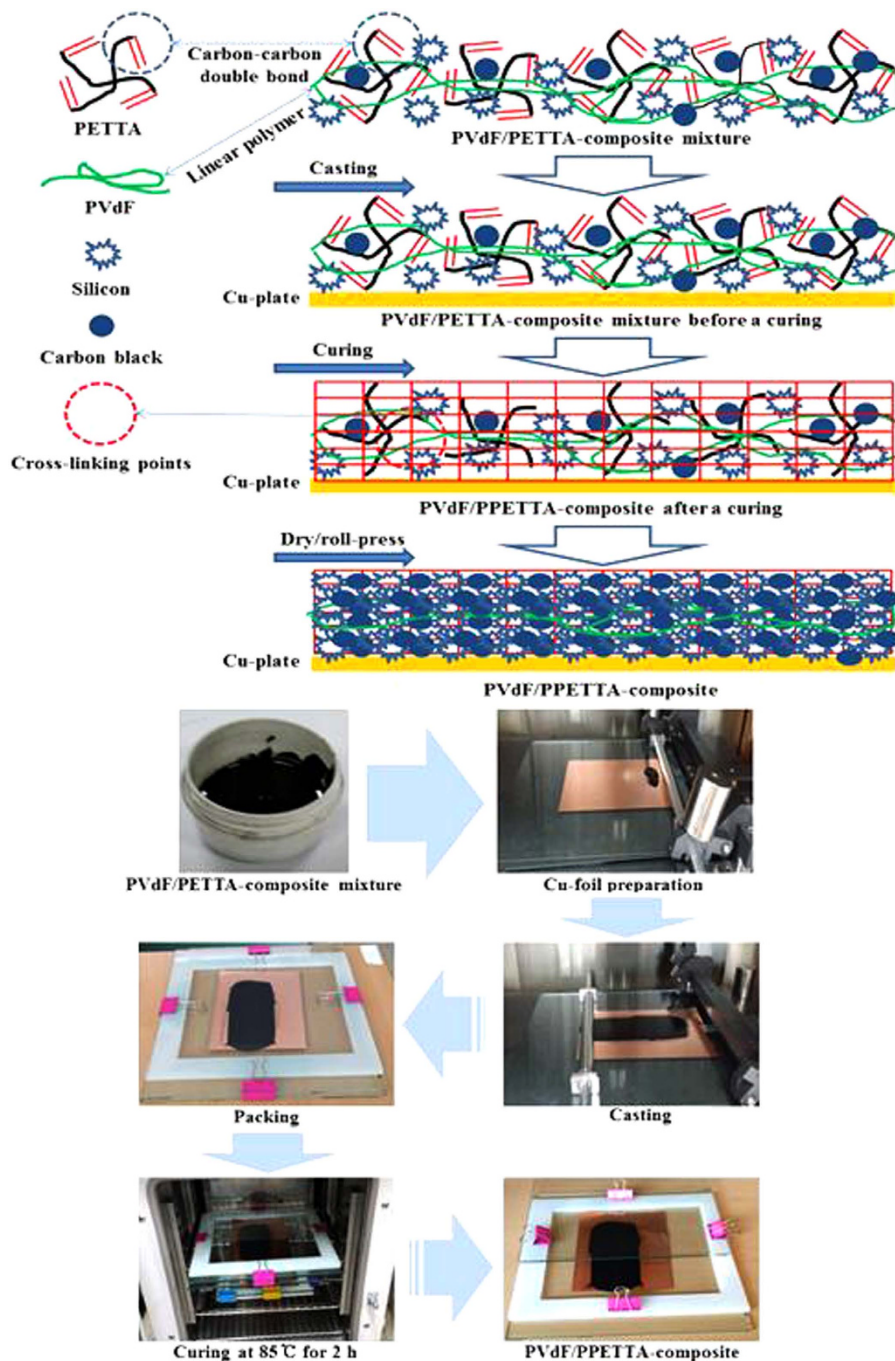
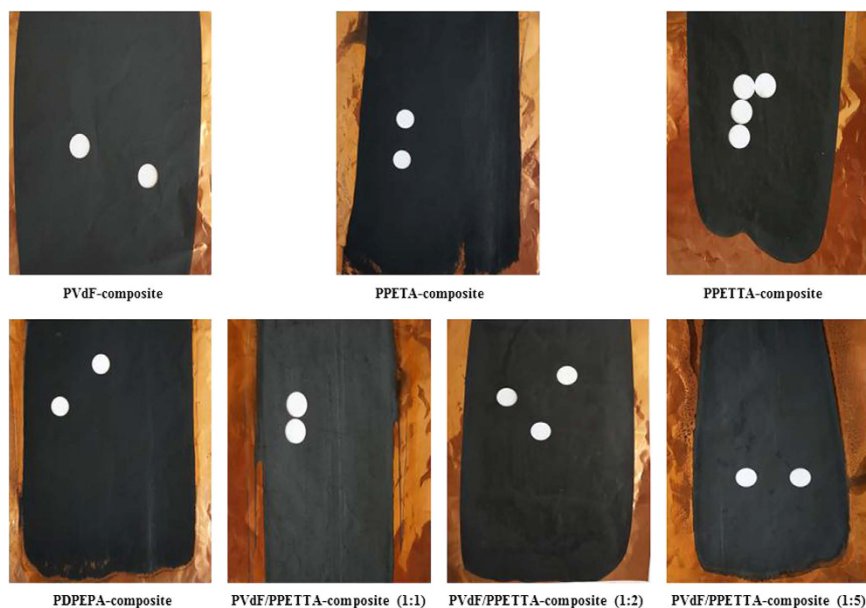


Figure 2. Fabrication process of the PVdF/PPETTA-composites.

Sample	Si	CB	PVdF	PETA	PETTA	DPEPA	AIBN	NMP	Curing
PVdF-composite	0.60 g	0.25 g	0.15 g	—	—	—	—	3.0 g	NO
PPETA-composite	0.60 g	0.25 g	—	0.15 g	—	—	0.005 g	3.0 g	YES
PPETTA-composite	0.60 g	0.25 g	—	—	0.15 g	—	0.005 g	3.0 g	YES
PDPEPA-composite	0.60 g	0.25 g	—	—	—	0.15 g	0.005 g	3.0 g	YES
PVdF/PPETTA-composite (1:1)	0.60 g	0.25 g	0.075 g	—	0.075 g	—	0.005 g	3.0 g	YES
PVdF/PPETTA-composite (1:2)	0.60 g	0.25 g	0.05 g	—	0.10 g	—	0.005 g	3.0 g	YES
PVdF/PPETTA-composite (1:5)	0.60 g	0.25 g	0.025 g	—	0.125 g	—	0.005 g	3.0 g	YES

Table 1. Materials for the fabrication of the PVdF-composite, PPETA-composite, PPETTA-composite, PDPEPA-composite and PVdF/PPETTA-composites.



**Figure 3.** Photographs of the PVdF-composite, PPETA-composite, PPETTA-composite, PDPEPA-composite and PVdF/PPETTA-composites.

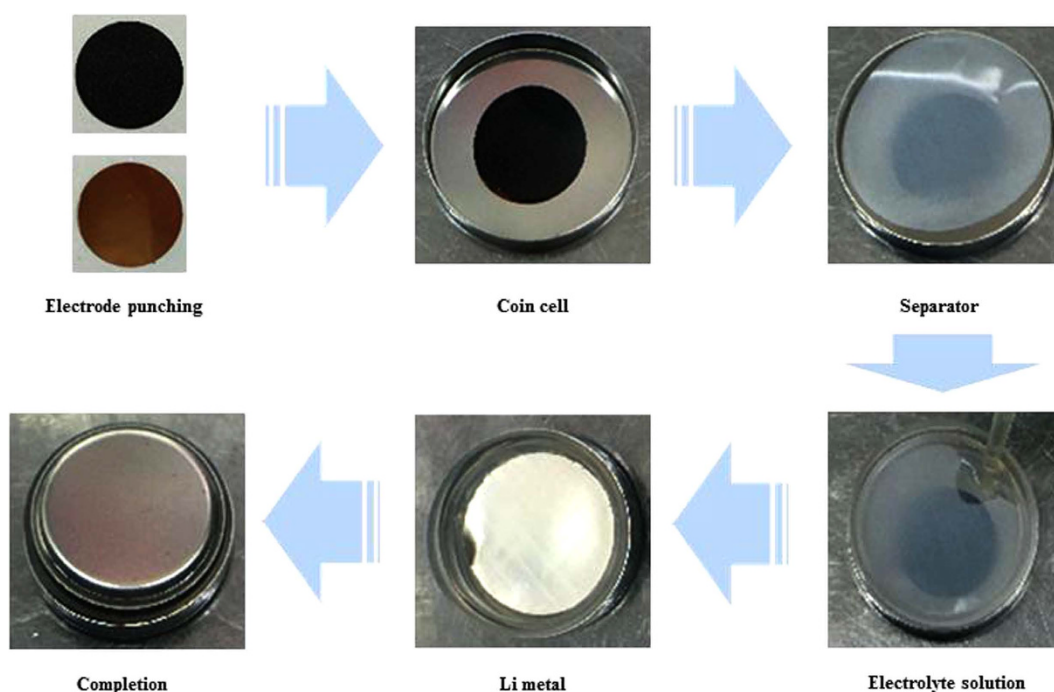


**Figure 4.** Cell production process used to create the composite electrodes.

**Electrochemical properties of the composite electrodes.** Figure 8(b) shows the cycle performance of the PVdF-composite, the PPETA-composite, the PPETTA-composite, the PDPEPA-composite and the PVdF/PPETTA-composites. The discharge of the PVdF-composite amounted to  $2359 \text{ mAh g}^{-1}$ , and it decreased by approximately 34% compared to the theoretical specific capacity of Si. In this case, the charge dropped sharply after one cycle, with only close to 8% (about  $202 \text{ mAh g}^{-1}$ ) of the discharge maintained after 15 cycles. Because the Li-ions migrate through the electrolyte-sorbed binder matrix<sup>5,7</sup>, it is expected that the poor electrolyte uptake of the PVdF decreased the discharge by reducing the number of Li-ionic carriers in the binder matrix. This occurred because the formation of an unstable solid electrolyte interphase (SEI) layer causes uninterrupted electrolyte solution degradation at the surface of the Si during the cycling process<sup>9–16</sup>. The abrupt reduction of the charge that occurred after one cycle can be attributed to the considerable volume expansion and the collapse of Si within



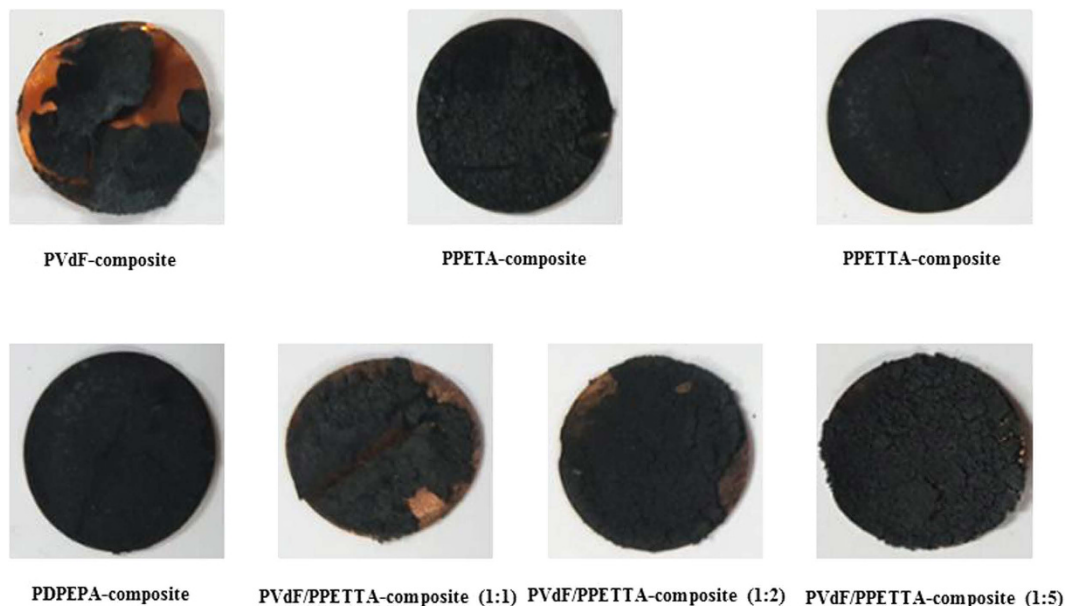


**Figure 5.** Images of the PVdF-composite, PPETA-composite, PPETTA-composite, PDPEPA-composite and PVdF/PPETTA-composites after 10 cycles.

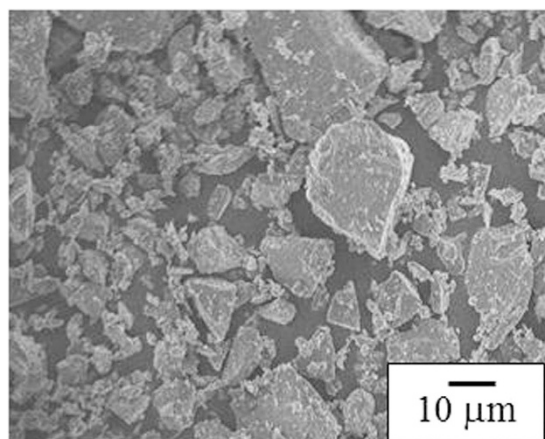


**Figure 6.** FE-SEM image of the Si particles used in this study.

Sample	PVdF	PETA	PETTA	DPEPA	AIBN	NMP	Curing	Casting	EU
raw-PVdF binder	1.5 g	—	—	—	—	15 g	NO	YES	18.9%
raw-PPETA binder	—	1.5 g	—	—	0.005 g	15 g	YES	NO	154.4%
raw-PPETTA binder	—	—	1.5 g	—	0.005 g	15 g	YES	NO	188.5%
raw-PDPEPA binder	—	—	—	1.5 g	0.005 g	15 g	YES	NO	98.2%
raw-PVdF/PPETTA (1:1) binder	0.75 g	—	0.75 g	—	0.005 g	15 g	YES	NO	26.7%
raw-PVdF/PPETTA (1:2) binder	0.5 g	—	1.0 g	—	0.005 g	15 g	YES	NO	39.4%
raw-PVdF/PPETTA (1:5) binder	0.25 g	—	1.25 g	—	0.005 g	15 g	YES	NO	60.5%

**Table 2.** Materials for the fabrication and the resulting EU of each raw binder.

the composite electrode<sup>1,2,15,16</sup>. As shown in Fig. 5, the surface cracks on the morphology of the PVdF-composite were much worse than on the other samples after 10 cycles. The PVdF-composite was nearly detached from the current collector.

On the other hand, the respective discharge amounts for the PPETA-composite, PPETTA-composite and PDPEPA-composite were approximately 1733 mAh g<sup>-1</sup>, 1921 mAh g<sup>-1</sup> and 1352 mAh g<sup>-1</sup>, with corresponding decreases of 51%, 46 and 62% compared to the theoretical specific capacity of Si. All cases showed much less

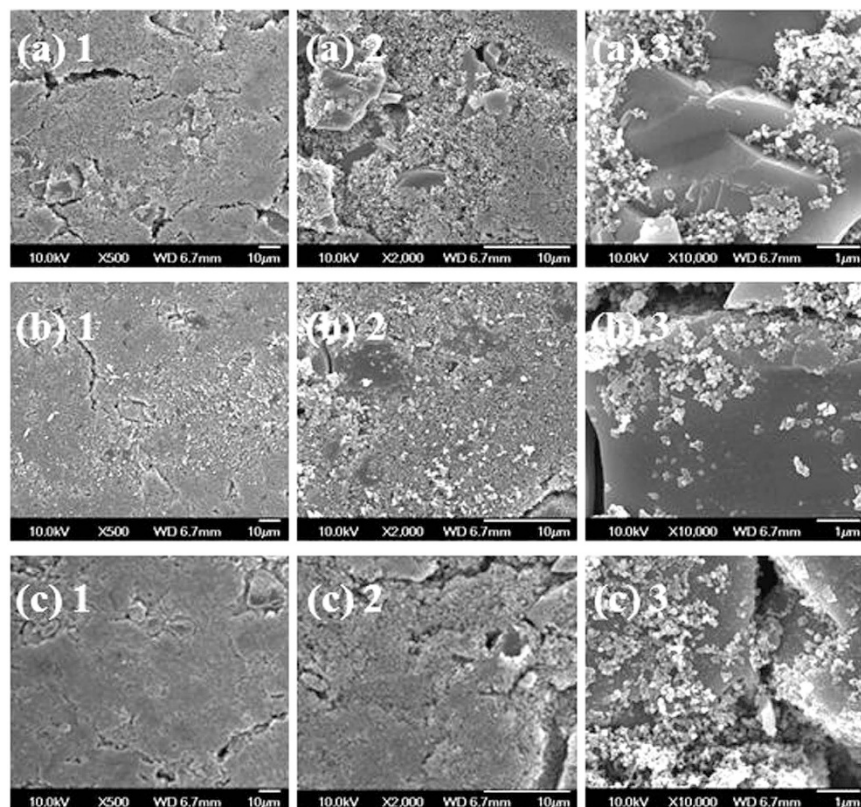


**Figure 7.** (a) FE-SEM images of the PVdF-composite, (b) the PPETTA-composite, and (c) the PVdF/PPETTA-composite (1:1).

discharge than the PVdF-composite. Despite the high electrolyte uptake of the cross-linked polymer binders, this most likely occurred because the excessive cross-linking networks of the PPETA, PPETTA and PDPEPA increased the amount of Li trapping by blocking the Li-ion channels in the binder matrix<sup>3,5,6,17</sup>. In that the cross-linked density increases with an increase in the number of carbon-carbon double bonds in a functional monomer<sup>6,8,13,17</sup>, we expect that the discharge of the PDPEPA-composite was decreased compared to those of the PPETA-composite and the PPETTA-composite. Nevertheless, the charge in these three corresponding cases remained at approximately 47% (about 818 mAh g<sup>-1</sup>) of the discharge, at approximately 53% (about 1022 mAh g<sup>-1</sup>) of the discharge, and at approximately 47% (about 636 mAh g<sup>-1</sup>) of the discharge for 15 cycles. These values are nearly, 4, 5 and 3 times higher than that of the PVdF-composite. Moreover, the PPETA-composite, PPETTA-composite and PDPEPA-composite showed much better surface morphologies than the PVdF-composite after 10 cycles (Fig. 5). Accordingly, we believe that the cross-linked polymer networks of PPETA, PPETTA and PDPEPA as binders played an important role through volume variation of Si and in maintaining the binding strength within the composite electrodes during the cycling process<sup>18–22</sup>. This could occur because the robust cross-linking binder system reduced the deformation of SEI layers and the mechanical stress of crystalline Li<sub>15</sub>Si<sub>4</sub> within the composite electrodes<sup>9–16</sup>.

The discharge amounts of the PVdF/PPETTA-composite (1:1), the PVdF/PPETTA-composite (1:2), and the PVdF/PPETTA-composite (1:5) were approximately 2739 mAh g<sup>-1</sup>, 3013 mAh g<sup>-1</sup> and 1897 mAh g<sup>-1</sup>, respectively, showing decreases of approximately 22%, 15 and 47% compared to the theoretical specific capacity of Si. Specifically, the discharge amounts of the PVdF/PPETTA-composite (1:1) and the PVdF/PPETTA-composite (1:2) improved remarkably by approximately 380 mAh g<sup>-1</sup> and 654 mAh g<sup>-1</sup> respectively, compared to that of the PVdF-composite. These outcomes can be attributed to the fact that the numbers of Li traps of the PVdF/PPETTA binder (1:1) and the PVdF/PPETTA binder (1:2) decreased as the volume of the cross-linked PPETTA domain in the binder matrix was reduced<sup>6,18,19</sup>. The charge in these respective cases remained at approximately 12% (about 337 mAh g<sup>-1</sup>) of the discharge, at about 24% (about 733 mAh g<sup>-1</sup>) of the discharge, and at nearly 46% (about 884 mAh g<sup>-1</sup>) of the discharge for 15 cycles, increasing with an increase in the content of the cross-linked PPETTA in the blending binder matrix. The entire charge pattern for the PVdF/PPETTA-composite (1:5) was similar to that of the PPETTA-composite during the cycling process. The charge patterns of the PVdF-composite, PPETA-composite, PPETTA-composite, PDPEPA-composite and PVdF/PPETTA-composites during the cycling process are shown in Table 3.

According to work by Dong *et al.*<sup>11</sup> the discharge amount of micro-Si negative electrodes for LIBs with sodium carboxymethyl cellulose (Na-CMC) as a binder was approximately 2150 mAh g<sup>-1</sup>, showing a decrease of 40% compared to the theoretical specific capacity of Si. The charge in this case was approximately 1770 mAh g<sup>-1</sup> after one cycle. Park *et al.*<sup>7</sup> also showed that (poly)vinyl alcohol (PVA) as a binder maintained excellent cyclic

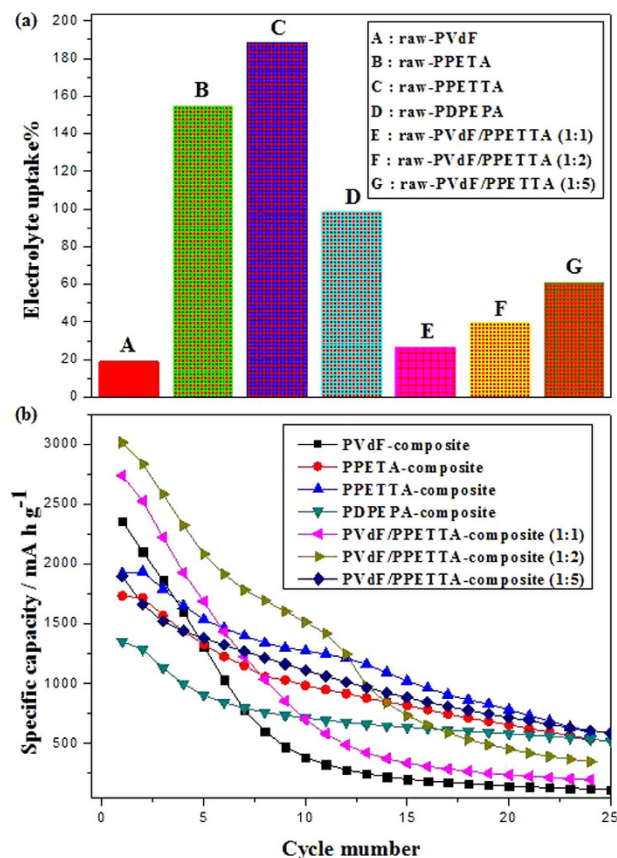


**Figure 8.** (a) EUs of the raw PVdF, PPETA, PPETTA, PDPEPA and PVdF/PPETTA binders and (b) cycle performance levels of the PVdF-composite, PPETA-composite, PPETTA-composite, PDPEPA-composite and PVdF/PPETTA-composites.

Sample	1 cycle	5 cycle	10 cycle	15 cycle	20 cycle	25 cycle
PVdF-composite	100%	55%	16%	8%	6%	4%
	(2359 mA h g <sup>-1</sup> )	(1312 mA h g <sup>-1</sup> )	(385 mA h g <sup>-1</sup> )	(202 mA h g <sup>-1</sup> )	(145 mA h g <sup>-1</sup> )	(116 mA h g <sup>-1</sup> )
PPETA-composite	100%	76%	56%	47%	37%	31%
	(1733 mA h g <sup>-1</sup> )	(1328 mA h g <sup>-1</sup> )	(985 mA h g <sup>-1</sup> )	(818 mA h g <sup>-1</sup> )	(655 mA h g <sup>-1</sup> )	(539 mA h g <sup>-1</sup> )
PPETTA-composite	100%	80%	66%	53%	40%	30%
	(1921 mA h g <sup>-1</sup> )	(1537 mA h g <sup>-1</sup> )	(1275 mA h g <sup>-1</sup> )	(1022 mA h g <sup>-1</sup> )	(784 mA h g <sup>-1</sup> )	(589 mA h g <sup>-1</sup> )
PDPEPA-composite	100%	66%	52%	47%	43%	38%
	(1352 mA h g <sup>-1</sup> )	(905 mA h g <sup>-1</sup> )	(712 mA h g <sup>-1</sup> )	(636 mA h g <sup>-1</sup> )	(583 mA h g <sup>-1</sup> )	(522 mA h g <sup>-1</sup> )
PVdF/PPETTA-composite (1:1)	100%	61%	25%	12%	8%	7%
	(2739 mA h g <sup>-1</sup> )	(1688 mA h g <sup>-1</sup> )	(701 mA h g <sup>-1</sup> )	(337 mA h g <sup>-1</sup> )	(237 mA h g <sup>-1</sup> )	(197 mA h g <sup>-1</sup> )
PVdF/PPETTA-composite (1:2)	100%	69%	50%	24%	15%	11%
	(3013 mA h g <sup>-1</sup> )	(2084 mA h g <sup>-1</sup> )	(1515 mA h g <sup>-1</sup> )	(733 mA h g <sup>-1</sup> )	(454 mA h g <sup>-1</sup> )	(348 mA h g <sup>-1</sup> )
PVdF/PPETTA-composite (1:5)	100%	72%	58%	46%	37%	32%
	(1897 mA h g <sup>-1</sup> )	(1377 mA h g <sup>-1</sup> )	(1112 mA h g <sup>-1</sup> )	(884 mA h g <sup>-1</sup> )	(716 mA h g <sup>-1</sup> )	(609 mA h g <sup>-1</sup> )

**Table 3.** Charge pattern of the PVdF-composite, PPETA-composite, PPETTA-composite, PDPEPA-composite and PVdF/PPETTA-composite during the cycling process.

retention of Si/graphites due to its numerous hydroxyl groups. The discharge amount for their Si/graphites negative electrode was approximately 1500 mA h g<sup>-1</sup>. Koo *et al.*<sup>6</sup> reported that the discharge amounts of Si composite electrodes with cured PAA-CMC, PAA and PVdF binders were approximately 2850 mA h g<sup>-1</sup>, 2200 mA h g<sup>-1</sup> and 300 mA h g<sup>-1</sup> respectively, at a current density of 300 mA g<sup>-1</sup>. As mentioned earlier, these studies depended only on a linear-polymer as a binder. The lower electrochemical performances reported in those studies may be due to the weak linear-polymeric binding system used or the poor electrolyte uptake levels of the binders within the Si negative electrodes in comparison to our study.



In conclusion, despite the fact that the charge of the PPETA-composite, the PPETTA-composite and the PDPEPA-composite as investigated here increased sharply during the cycling process, the discharge in these cases dropped significantly compared to that of the PVdF-composite. These outcomes were improved considerably by blending a linear-polymer binder and a cross-linked polymer binder through a curing process. These results could stem from the precise manipulation of the electrolyte uptake and cross-linking level of the binder within the composite electrodes.

## Methods

**Materials.** Si was purchased from Aldrich and used as received (powder, –325 mesh, 99% trace metals basis). PETA (molecular formula:  $C_{14}H_{18}O_7$ , Mw: 298.24, CAS number: 3524-68-3, density: 1.18 g/mL at 25 °C (lit.), Refractive index:  $n_{20/D}$  1.483 (lit.), Flash point: >230 °F), PETTA (molecular formula:  $C_{17}H_{20}O_8$ , Mw: 352.34, CAS number: 4986-89-4, density: 1.19 g/mL at 25 °C (lit.), Refractive index:  $n_{20/D}$  1.487 (lit.), Flash point: >230 °F), DPEPA (molecular formula:  $C_{25}H_{32}O_{12}$ , Mw: 524.52, CAS number: 60506-81-2, density: 1.155 g/mL at 25 °C (lit.), Refractive index:  $n_{20/D}$  1.49 (lit.), Flash point: >230 °F), CB (Denka black) and NMP (molecular formula:  $C_5N_9NO_2$ , Mw: 115.13, CAS number: 41194-00-7) were also purchased from Aldrich and used as received. AIBN (molecular formula:  $C_8H_{12}N_4$ , Mw: 164.21, CAS number: 78-67-1) was purchased from DEEJUNG CHEMICALS & METALS CO., LTD.

**Coin half-cell measurements.** Coin half cells (CR2032) were manufactured in a dry glove box with ethylene carbonate (EC)/ethyl methyl carbonate (EMC) (3:7 vol. ratio) as an electrolyte containing 1.3 M of  $LiPF_6$  and Celgard® commercial trilayer PP/PE/PP separators. Lithium metal was used as a counter electrode. The galvanostatic cycle was carried out in a voltage range of 0~2.0 V with a current density of 100 mA/g (WBCS 3000 cycler, Wonatech Co., Korea).

**EU measurement.** The EU of the prepared raw-binders was determined by measuring the change in the weight between the wet and dry binder. The raw-binders were soaked in an EC/EMC (3:7 vol. ratio) electrolyte solution containing 1.3 M of  $LiPF_6$  at room temperature for 48 h. The external electrolyte was wiped off, and the binders were weighed. The electrolyte uptake amounts of the binders were obtained by the following equation:

$$EU = \frac{W_{wet} - W_{dry}}{W_{dry}} \times 100\%$$

Here,  $W_{dry}$  and  $W_{wet}$  are the weight of the dried and the electrolyte-sorbed binder, respectively.

**Morphology measurement.** Dispersed electrode particle images of the prepared electrodes were confirmed by a field emission scanning electron microscope (FE-SEM, Hitachi Co. Japan).

## References

- Ito, K. Novel cross-linking concept of polymer Network: synthesis, structure, and properties of slide-ring gels with freely movable junctions. *Polym. J.* **39**, 489–499 (2007).
- Tillet, G., Boutevin, B. & Ameduri, B. Chemical reactions of polymer crosslinking and post crosslinking at room and medium temperature. *Prog. Polym. Sci.* **36**, 191–217 (2011).
- Kim, J. Y. *et al.* Preparation of organic–inorganic nanocomposite membrane using a reactive polymeric dispersant and compatibilizer: Proton and methanol transport with respect to nano-phase separated structure. *J. Membr. Sci.* **283**, 172–181 (2013).
- Kim, J. Y. *et al.* Synthesis of CdS nanoparticles dispersed within solutions and polymer films using amphiphilic urethane acrylate chains. *J. Ind. Eng. Chem.* **15**, 103–109 (2009).
- Jang, S. Y. & Han, S. H. Characterization of sulfonated polystyrene-block-poly(ethyl-ran-propylene)-block-polystyrene copolymer for proton exchange membranes (PEMs). *J. Membr. Sci.* **444**, 1–8 (2013).
- Koo, B. *et al.* A highly cross-linked polymeric binder for high-performance silicon negative electrodes in lithium ion batteries. *Angew. Chem. Int. Ed.* **51**, 8762–8767 (2012).
- Park, H. K. *et al.* Effect of high adhesive polyvinyl alcohol binder on the anodes of lithium ion batteries. *Electrochem. Commun.* **13**, 1051–1053 (2011).
- Ahn, S. H. *et al.* Synthesis and characterization of soluble polythiophene derivatives containing electron-transporting moiety. *Macromolecules* **34**, 2522–2527 (2001).
- Kovalenko, I. *et al.* A major constituent of brown algae for use in high-capacity Li-ion batteries. *Science* **334**, 75–79 (2011).
- Ryu, J. H. *et al.* The failure modes of silicon powder negative electrode in lithium secondary batteries. *Electrochem. Solid-State Lett.* **7**, A306–A309 (2004).
- Ding, N. *et al.* Improvement of cyclability of Si as anode for Li-ion batteries. *J. Power Sources* **192**, 644–651 (2009).
- Ji, X. *et al.* A highly ordered nanostructured carbon–sulphur cathode for lithium–sulphur batteries. *Nature Materials* **3**, 500–506 (2009).
- Chen, Z. *et al.* Large-volume-change electrodes for Li-ion batteries of amorphous alloy particles held by elastomeric tethers. *Electrochem. Commun.* **5**, 919–923 (2003).
- Li, J. *et al.* Lithium polyacrylate as a binder for tin–cobalt–carbon negative electrodes in lithium-ion batteries. *Electrochim. Acta.* **55**, 2991–2995 (2010).
- Buqa, H. *et al.* Study of styrene butadiene rubber and sodium methyl cellulose as binder for negative electrodes in lithium-ion batteries. *J. Power Sources* **161**, 617–622 (2006).
- Komab, S. *et al.* Polyacrylate modifier for graphite anode of lithium-ion batteries. *Electrochem. Solid-State Lett.* **12**, A107–A110 (2009).
- Sato, K. & Koinuma, H. Highly cross-linked polymer networks of amorphous silicon alloys quantum chemical studies on plasma and photochemical processes. *Prog. Polym. Sci.* **21**, 255–297 (1996).
- Wu, M. *et al.* Toward an ideal polymer binder design for high-capacity battery anodes. *J. Am. Chem. Soc.* **135**, 12048–12056 (2013).
- Sagar, R. U. R. *et al.* High capacity retention anode material for lithium ion battery. *Electrochim. Acta.* **211**, 156–163 (2016).
- Nguyen, M. H. T. & Oh, E. S. Application of a new acrylonitrile/butylacrylate water-based binder for negative electrodes of lithium-ion batteries. *Electrochem. Commun.* **35**, 45–48 (2013).



21. Xue, Z., Zhang, Z. & Amine, K. Cross-linkable urethane acrylate oligomers as binders for lithium-ion battery. *Electrochem. Commun.* **34**, 86–89 (2013).
22. Tsao, C. H., Hsu, C. H. & Kuo, P. L. Ionic conducting and surface active binder of poly(ethylene oxide)-block-poly(acrylonitrile) for high power lithium-ion battery. *Electrochim. Acta.* **196**, 41–47 (2016).

### Author Contributions

First author (Dr. Suk-Yong Jang) wrote the main manuscript text and corresponding author (Prof. Dr. rer. nat. Sien-Ho Han) prepared figures. All authors reviewed the manuscript.

### Additional Information

**Competing financial interests:** The authors declare no competing financial interests.

**How to cite this article:** Jang, S.-Y. and Han, S.-H. Fabrication of Si negative electrodes for Li-ion batteries (LIBs) using cross-linked polymer binders. *Sci. Rep.* **6**, 38050; doi: 10.1038/srep38050 (2016).

**Publisher's note:** Springer Nature remains neutral with regard to jurisdictional claims in published maps and institutional affiliations.



This work is licensed under a Creative Commons Attribution 4.0 International License. The images or other third party material in this article are included in the article's Creative Commons license, unless indicated otherwise in the credit line; if the material is not included under the Creative Commons license, users will need to obtain permission from the license holder to reproduce the material. To view a copy of this license, visit <http://creativecommons.org/licenses/by/4.0/>

© The Author(s) 2016